Journal of Molecular Liquids 185 (2013) 36–43

Contents lists available at SciVerse ScienceDirect

Journal of Molecular Liquids

journal homepage: www.elsevier.com/locate/molliq

Modelling and understanding of the vapour–liquid and liquid–liquid interfacial properties for the binary mixture of *n*-heptane and perfluoro-*n*-hexane

Hector Domínguez [a,*], Andrew J. Haslam [b], George Jackson [b], Erich A. Müller [b]

[a] Instituto de Investigaciones en Materiales, Universidad Nacional Autónoma de México, D.F. 04510, Mexico
[b] Department of Chemical Engineering, Imperial College London, South Kensington Campus, London SW7 2AZ, United Kingdom

ARTICLE INFO

Available online 12 October 2012

Keywords:
Molecular dynamics
Interfacial tension
Aneotropy
SAFT
Phase equilibria

ABSTRACT

A detailed molecular-dynamics (MD) simulation study of the interfacial tension of the *n*-heptane + perfluoro-*n*-hexane ($C_6F_{14} + C_7H_{16}$) binary mixture is carried out at different temperatures and compositions for the vapour–liquid and liquid–liquid interfaces. The molecules are represented as chains of united-atom segments using previously reported force-field pure-component parameters with no further modification, while the unlike interaction energy between the alkyl and perfluoroalkyl segments is adjusted to describe the experimental data for the fluid phase equilibria. In the case of the vapour–liquid interface a horizontal inflection at a critical composition, sometimes referred to as aneotropy, is represented by our model as found in experimental work. Interfacial tensions for both the liquid-liquid and vapour-liquid interfaces are determined using the test-area method. A prerequisite of the determination of the interfacial tension by direct MD simulation involves studies of the fluid phase equilibria (vapour–liquid (VLE) and liquid–liquid equilibria (LLE)). A unique unlike energetic interaction parameter is adjusted to improve the prediction of the LLE and used in all the other simulations. The resulting description of the fluid phase behaviour is compared with that calculated using an equation of state (SAFT), and with experimental data where available; good agreement is observed.

1. Introduction

Although perfluoroalkanes and alkanes appear similar from the point of view of their molecular structure, they exhibit very different physical properties. For example, mixtures of these components display substantial deviations from ideality as evidenced in a variety of interesting phenomena, including large regions of liquid–liquid immiscibility, large positive deviations from Raoult's law, and large positive excess functions [1,2]. Another physical property of particular interest in perfluoroalkane + alkane mixtures is the interfacial tension: isotherms of the vapour–liquid interfacial tension of these mixtures present a horizontal inflection close to the critical composition [3,4], as predicted by the square gradient theory of van der Waals [5,6]: moreover, the interfacial tension isotherms close to the critical region are found to be characterised by a variety of shapes, some of which suggest aneotropic behaviour [3,4]. Correspondingly, a large number of investigations have been carried out to address the unusual properties observed in these systems [7–16]; it has been suggested that the anomalous behaviour could be the result of an unusually weak attractive interaction between the alkyl and perfluoroalkyl moieties.

One approach to investigating perfluoroalkane + alkane mixtures is to model them using equations of state (EoSs). In particular, over the last few decades a new generation of EoSs based on the statistical associating fluid theory (SAFT) have proved to be reliable in the study of a variety of fluid systems, such as polymers, polar and hydrogen-bonding fluids, electrolytes, etc. [17–22]. The SAFT approach has also proven to be successful in the study of mixtures comprising alkanes and/or perfluoroalkanes, and several studies of these systems, using different versions of the SAFT EoS, have been reported [2,23–37].

Another approach to investigating perfluoroalkane + alkane mixtures is the direct representation of the molecules with specific force fields using computer simulation. Computer-simulation techniques now provide a powerful alternative tool for the investigation of such interfacial systems. A particularly attractive feature of these techniques is that they can help us understand the systems from a molecular perspective. However, only a limited number of studies have been reported for alkane + perfluoroalkane systems [38–42].

In our current work we employ both the SAFT EoS and computer simulation to study perfluoroalkane + alkane mixtures, exemplified by the *n*-heptane + perfluoro-*n*-hexane system (for which some work has been previously reported [43,44]). The fluid phase equilibria calculated with the theory and simulation are compared with the available experimental data. However, we concentrate mainly on the computer-simulation aspect of the work: there are only limited examples of the use of the so-called test-area perturbation method for the determination of the interfacial tension of two high-density fluid states [45–49] analysing both vapour–liquid and liquid–liquid

* Corresponding author.
E-mail addresses: hectordc@unam.mx (H. Domínguez), g.jackson@imperial.ac.uk (G. Jackson).

0167-7322/$ – see front matter
http://dx.doi.org/10.1016/j.molliq.2012.09.011

interfaces. Liquid–liquid interfacial tensions have been calculated by molecular simulations in a number of studies [40,50–63]. In our work, the first computational study of the vapour–liquid and liquid–liquid interfacial tensions for the *n*-heptane + perfluoro-*n*-hexane mixture is undertaken, the latter also representing (to the best of our knowledge) the first reports of the liquid–liquid interfacial tension for this system.

2. Computational method and model

Simulations of the binary mixture of *n*-heptane and perfluoro-*n*-hexane are undertaken in the *NVT* ensemble using the molecular-dynamics method with a Nosé–Hoover thermostat [64]. The total potential energy comprises inter- and intramolecular interactions. The intermolecular interactions between the molecular segments are described using the Lennard-Jones potential with the *n*-heptane parameters taken from reference [65] and the perfluoro-*n*-hexane parameters from reference [41]. The intramolecular potential comprises bond, angular and torsional interactions:

The bond-stretching potential is calculated with a harmonic potential,

$$E_{bond} = \frac{K_b}{2}(r - r_0)^2 \tag{1}$$

where r_0 is the equilibrium distance between the two bonded atoms and K_b is the bond constant.

The bond-bending interaction is also represented using a harmonic potential,

$$E_{ang} = \frac{K_\theta}{2}(\theta - \theta_0)^2 \tag{2}$$

where θ_0 is the equilibrium angle and K_θ is the corresponding force constant.

The dihedral (torsional) potential for the alkane is modelled with the OPLS-UA potential [66],

$$E_{dih} = c_0 + c_1[1 + \cos(\phi)] + c_2[1 - \cos(2\phi)] + c_3[1 + \cos(3\phi)] \tag{3}$$

where the c_k are the energy constants and ϕ is the dihedral angle.

In the case of the perfluoroalkanes, the torsional potential suggested by Cui et al. [67] is used

$$E_{dih} = \sum_{k=0}^{7} \chi_k \cos^k(\phi) \tag{4}$$

where the χ_k are again constants which characterise the interaction. The complete set of pure-component parameters used in our simulations is given in Tables 1 and 2.

For the unlike intermolecular segment–segment interactions between molecules of the different species, the well-known Lorentz-Berthelot combining rules are commonly used:

$$\sigma_{ij} = \frac{1}{2}\left(\sigma_{ii} + \sigma_{jj}\right) \quad \text{(Lorentz)}; \tag{5}$$

$$\epsilon_{ij} = \sqrt{\epsilon_{ii}\epsilon_{jj}} \quad \text{(Berthelot)}, \tag{6}$$

where σ represents the size parameter and ϵ the energy parameter of the intermolecular potential (see Table 1).

It has long been known that the unlike intermolecular interaction between alkyl and perfluoroalkyl groups required to adequately describe perfluoroalkane + alkane mixtures deviates substantially from the Berthelot (geometric-mean) rule, as investigated early on by Hudson and McCoubrey [68]. Consistent with this, large deviations from the Berthelot rule have been found in several modelling studies [16,25–27,69–71]. Since the seminal work of Hudson and McCoubrey [68], the role of unlike intermolecular-potential parameters in mixtures has been addressed in numerous papers; for a review see [72]. Based on these findings, large deviations from the Berthelot rule are, indeed, to be expected on theoretical grounds for these mixtures. Accordingly, for the unlike alkane-perfluoroalkane inter-molecular interaction a deviation parameter is used in our work to correct the value obtained with the Berthelot rule:

$$\epsilon_{ij} = \left(1 - k_{ij}\right)\sqrt{\epsilon_{ii}\epsilon_{jj}} \tag{7}$$

Different values of the deviation parameter k_{ij} are examined in the simulations and it is found that $k_{ij} = 0.1$ provides the best agreement with the experimental data for the liquid–liquid immiscibility.

Molecular-dynamics simulations of the liquid–liquid equilibria are started from an initial configuration consisting of two adjacent slabs of pure *n*-heptane and perfluoro-*n*-hexane molecules located in a rectangular box. Isothermal–isobaric (*NpT*-ensemble) simulations are then carried out at a pressure corresponding to the liquid phase to equilibrate the system and establish the equilibrium box dimension to be used in the subsequent canonical (*NVT*-ensemble) simulations; dimensions of $X = Y = 42.989$ Å and $Z = 193.889$ Å are thereby chosen. The system is then simulated in the *NVT* ensemble at different temperatures up to the critical region.

For simulations of the vapour–liquid equilibria nine systems are studied, corresponding to each of the pure components and seven different mixtures across the composition range. Initial configurations

Table 1
Intramolecular and intermolecular potential parameters.

Nonbonded interactions		
Group	ϵ(kJ/mol)	σ(Å)
CH_3	0.8647	3.91
CH_2	0.3808	3.93
CF_3	0.7234	4.36
CF_2	0.2286	4.73
Bond stretching		
	r_o(Å)	K_b(kJ/mol Å^2)
$CH_x - CH_y$	1.54	802.3465
$CF_x - CF_y$	1.54	802.3465
Bond bending		
	θ_0(deg)	K_θ(kJ/mol rad^2)
$CH_x - (CH_2) - CH_y$	114	519.6545
$CF_x - (CF_2) - CF_y$	114	519.6545

Table 2
Contact for the diheral (torsional) potentials.

Parameter	Value (K)
Alkane torsion (Eq. (3))	
c_0/k_B	0
c_1/k_B	335.03
c_2/k_B	−68.19
c_3/k_B	791.32
Perfluoroalkane torsion (Eq. (4))	
χ_0/k_B	940.4
χ_1/k_B	−282.7
χ_2/k_B	1355.2
χ_3/k_B	6800.0
χ_4/k_B	−7875.3
χ_5/k_B	−14168.0
χ_6/k_B	9213.7
χ_7/k_B	4123.7

are obtained by placing molecules randomly in a simulation box of dimensions $X = Y = 43.0$ Å and $Z = 300.0$ Å.

All molecular-dynamics simulations are carried out in the *NVT* ensemble using the DL-POLY package [73] with a time step of 0.005 ps using the Hoover–Nosé thermostat [64] with a relaxation time of 0.1 ps. The usual periodic boundary conditions in all three directions are employed and the Lennard-Jones interactions are cut off at 15 Å. Finally, simulations up to 10 ns are conducted, using the last 4 ns for data acquisition.

3. The statistical associated fluid theory (SAFT)

To aid the molecular-dynamics simulation study of the fluid phase equilibria, phase diagrams for the *n*-heptane + perfluoro-*n*-hexane mixture are calculated using the SAFT EoS.

The SAFT approach [74,75] provides a versatile and accurate tool to study complex fluid phase behaviour. The approach stems from the first-order thermodynamic perturbation theory (TPT1) of Wertheim [76–79], which provides rigorous expressions for the free-energy contributions of associating chain fluids. Since the original version of the theory appeared, a number of modifications and extensions have been presented in which different forms of the intermolecular potential are employed and the structure of the reference fluid is treated in more detail (for reviews see, e.g., references [17–22]).

In the SAFT formalism, the free energy of a mixture of chain molecules is written as

$$\frac{F}{Nk_BT} = \frac{F^{ideal}}{Nk_BT} + \frac{F^{mono}}{Nk_BT} + \frac{F^{chain}}{Nk_BT} + \frac{F^{assoc.}}{Nk_BT} \tag{8}$$

where N is the number of molecules, and k_B is Boltzmann's constant. The terms on the right hand side of Eq. (8) represent individual contributions to the free energy. The first term, F^{ideal}, is the ideal free energy. F^{mono} is the contribution to the free energy due to the monomer–monomer interactions; in the version of SAFT for potentials of variable range (SAFT-VR) that we employ here this is obtained from a high-temperature perturbation expansion up to second order [80,81]. These first two terms alone would represent an equation of state of the van der Waals type, for attracting spherical molecules. F^{chain} is the contribution to the free energy of forming chains of m tangentially bonded spherical monomer segments, thereby introducing the effect of molecular shape into the EoS. F^{assoc} is the contribution due to molecular association; since neither alkanes nor perfluoroalkanes are associating molecules, in our current work no association contribution is included (i.e., $F^{assoc} = 0$).

Here SAFT-VR [80,81] is employed to model the fluid phase equilibria of the *n*-heptane + perfluoro-*n*-hexane mixture. In this approach an attractive potential of variable range and arbitrary shape is considered; for simplicity and ease of computation we choose the square-well potential, thereby molecules are modelled as chains of m spherical segments of diameter σ, interacting with each other through a square-well potential of depth ϵ and range λ. Moreover, in the theory the chain molecules are assumed to be fully flexible so there is no explicit orientation dependence in the interactions between the chains. However, it is worth noting that within the Wertheim TPT1 approach it is not possible to distinguish between fully flexible or rigid chains. The introduction of the additional non-conformal range parameter, λ, provides an added advantage in dealing with the challenging interactions of the perfluoroalkanes in an effective way. Although the analysis carried out in the current paper is for segment–segment interactions of the square-well form, the SAFT-VR approach is generic and has been developed for Yukawa [82], Lennard-Jones [83], and Mie [84] segment–segment interactions.

As for the molecular simulations, the representation of mixtures requires the determination of both the pure and the unlike intermolecular parameters. The pure-component parameters for the square-well models are taken from the literature [85,86]. Mixture combining rules of the form of Eqs. (5) and (7) were used to evaluate the unlike ϵ_{ij} parameters. Following Morgado et al. [2], an extra adjustable parameter (Γ_{ij}) is introduced to refine the unlike square-well range parameter:

$$\lambda_{ij} = \Gamma_{ij}\frac{\lambda_{ii}\sigma_{ii} + \lambda_{jj}\sigma_{jj}}{\sigma_{ii} + \sigma_{jj}}. \tag{9}$$

The complete set of SAFT-VR pure-component parameters for the chains of square-well segments used in this work is given in Table 3. The adjustable unlike square-well parameters used to describe the mixtures are $k_{ij} = 0.195$ and $\Gamma_{ij} = -0.06$.

4. Interfacial tension: the test-area method

The vapour–liquid and the liquid–liquid interfacial tensions are determined for the binary mixture from the direct molecular-dynamics simulation of the fluid interfaces. The traditional method to evaluate this quantity is the mechanical approach by calculating the components of the pressure tensor [87]; in our current work, however, a perturbative approach, known as the test-area (TA) [88] method is used. The TA method is a thermodynamic route via which the interfacial tension γ can be computed by generating infinitesimal perturbations in the interfacial area, thereby inducing small changes in the Helmholtz free energy of the system. In the *NVT* ensemble the expression for γ is given by [88]

$$\gamma = \left(\frac{\partial F}{\partial A}\right)_{NVT} = \lim_{\Delta A\to 0}\left(\frac{\Delta F}{\Delta A}\right)_{NVT} = -\frac{k_BT}{2\Delta A}\ln\left\langle \exp\left(\frac{-\Delta U}{K_BT}\right)\right\rangle. \tag{10}$$

Here, $\Delta A = A_1 - A_0$ is the infinitesimal perturbation in the area (A_0 is the unperturbed area and A_1 is the new area after perturbation), and $\Delta U = U_1 - U_0$ is the change in configurational energy. The factor of 1/2 is included because there are two interfaces in the simulated systems. Since the partial derivatives are carried out at constant volume (Eq. (10)) the perturbation in the area is obtained by the following transformations in the box dimensions: $X_1 = X_0\sqrt{1+\psi}$, $Y_1 = Y_0\sqrt{1+\psi}$ and $Z_1 = Z_0/(1+\psi)$ such that $V_1 (= X_1Y_1Z_1) = V_0 (= X_0Y_0Z_0)$, where ψ is a small perturbation parameter. For these calculations the system is monitored over 500 000 steps by performing the area change (both $\Delta A > 0$ and $\Delta A < 0$) every 10 steps. In each case the energy of the system is stored and, at the end of the simulation, the interfacial tension is calculated using Eq. (10) by averaging data generated from both increasing and decreasing the area. Different values of the parameter ψ are tested until γ is found to be essentially constant for the given range of ψ values. A value within this range, $\psi = 1\times10^{-5}$, is used as the perturbation parameter in all of the simulations to calculate the interfacial tensions.

5. Results

5.1. Fluid phase behaviour

The liquid–liquid equilibria (LLE) of the binary mixture are examined first. Simulations are conducted for 500 molecules of perfluoro-*n*-hexane and 750 molecules of *n*-heptane. The coexistence compositions are estimated from the density profiles calculated in two different

Table 3
SAFT-VR square-well segment parameters.

	C_7H_{16} [19]	C_6F_{14} [85]
m	3.0	2.85
λ	1.5574	1.432
σ(Å)	3.9567	4.456
ϵ/k_B(K)	253.28	283.1

ways. The first approach involves the calculation of the density profiles $\rho(Z)$ perpendicular to the interface (in the Z-direction), and the second by calculating the density of each species within a large number of spherical cells randomly inserted in the simulation box. The mole fraction of each species and the total density are then calculated and stored in histograms for the probability distributions of mole fraction [89]. In Fig. 1 the temperature-composition T–x LLE phase diagram for n-hexane + perfluoro-n-hexane is shown; here the simulated values are compared with two sets of available experimental data [43,44]. At low temperatures good agreement with experiment is observed, however, at temperatures close to the critical point slight deviations are apparent.

In the same figure, the corresponding representation with the SAFT-VR EoS is shown. As suggested by Morgado et al. [2], the inclusion of a negative value of the parameter for the range of the unlike square-well interaction Γ_{ij} (in Eq. (9)) is necessary to reproduce the unusual width of the liquid–liquid phase boundary exhibited by the n-heptane + perfluoro-n-hexane mixture. Indeed, a refinement of the unlike range (cf. Γ_{ij} in Eq. (9)) leads to a broader coexistence envelope than only adjusting the unlike attractive energy (cf. k_{ij} in Eq. (7)). However, it is worth noting that the use of a negative Γ_{ij} (in place of the usual $\Gamma_{ij}=0$) naturally leads to a larger (positive) value for k_{ij}, as was demonstrated in reference [72]. We use values of the unlike interaction parameters of $k_{ij}=0.195$ and $\Gamma_{ij}=-0.06$ to give the best description of the experimental LLE data, and these parameters are retained for all subsequent calculations. In large part, the reason that a negative Γ_{ij} leads to a large (positive) k_{ij} is that the integrated energy (van der Waals attractive constant) α_{ij}, given for the SW potential by $\alpha_{ij}=(2\pi/3)\epsilon_{ij}\sigma_{ij}^3(\lambda_{ij}^3-1)$, thereby takes approximately the same value. Accordingly, although the similar values of k_{ij} obtained in our current work and in reference [2] are rather larger than the value of $k_{ij}=0.08$ obtained by McCabe et al. [27] for alkane + perfluoroalkane mixtures (treated also within the SAFT-VR approach using a square-well potential), this simply reflects the choice of $\Gamma_{ij}=0$ made by McCabe et al. [27]. In common with the direct molecular dynamics simulation, the SAFT-VR EoS provides a good description of the experimental data at low temperature, however, as expected, the agreement becomes poorer as one approaches the critical region.

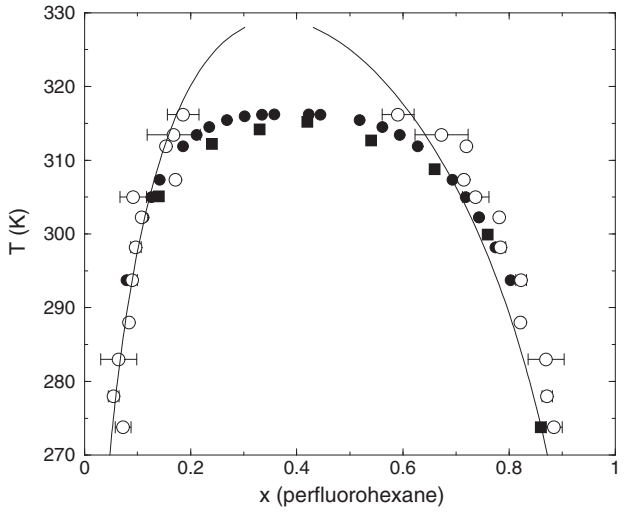

Fig. 1. The liquid–liquid equilibria (LLE) for the n-heptane + perfluoro-n-hexane binary mixture. The filled circles and squares are experimental data taken from references [44] and [43], respectively. The open circles represent data obtained from direct molecular dynamics simulation and the continuous curves are the representation with the SAFT-VR equation of state.

It is well known that analytical equations of state cannot simultaneously describe both the sub-critical and critical regions. The pure-component models are developed to capture the sub-critical region, thereby leading to an overprediction of the critical points; this is also reflected in the overprediction of the mixture critical line and, correspondingly, the temperature of the predicted liquid–liquid critical point of the mixture in Fig. 1 is too high.

The vapour–liquid equilibria (VLE) are also modelled using both molecular-dynamics simulation and the SAFT-VR EoS, using the same parameters as those used to describe the LLE. Simulations of the VLE region are undertaken at different compositions (using 1000 particles in total) at three different temperatures, ($T=298.15$, 317.65 and 328.15 K), which correspond to temperatures below, close to, and above the experimental liquid-liquid critical point.

The McCabe–Thiele representation of the vapour (y) and liquid (x) compositions for the n-heptane + perfluoro-n-hexane binary mixture at $T=298.15$, 317.65 and 328.15 K are shown in Fig. 2. In all cases s-shaped curves are observed, and at low temperatures the simulated data are seen to be in good agreement with the experimental data; as the temperature is increased, however, slight deviations are observed.

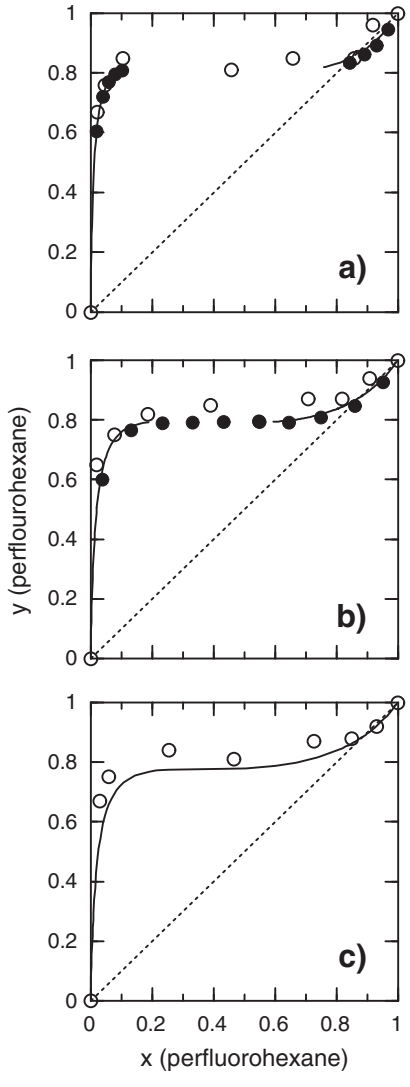

Fig. 2. The vapour–liquid equilibria (VLE) depicted in a McCabe–Thiele representation of the vapour (y) and liquid (x) compositions for the n-heptane + perfluoro-n-hexane mixture at a) $T=298.15$ K, b) $T=317.65$ K and c) 328.15 K. The filled circles are experimental data from reference [44], the open circles are the data obtained from direct molecular dynamics simulation, and the continuous curves represent the predictions with the SAFT-VR EoS.

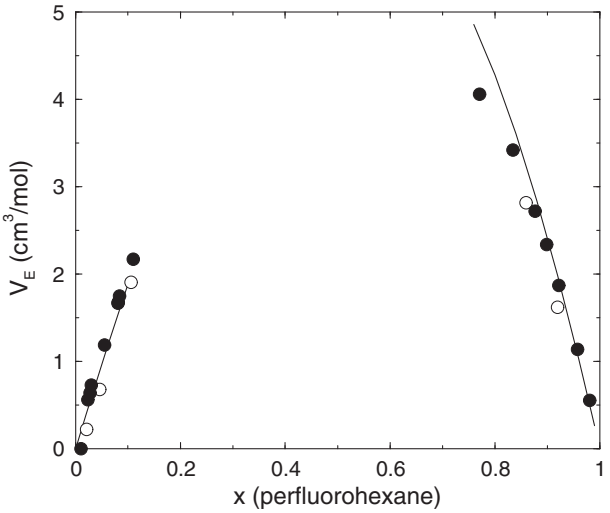

Fig. 3. The excess volumes for the *n*-heptane + perfluoro-*n*-hexane mixture at $T=298.15$ K. The experimental data are from reference [1]. See the legend of Fig. 2 for details.

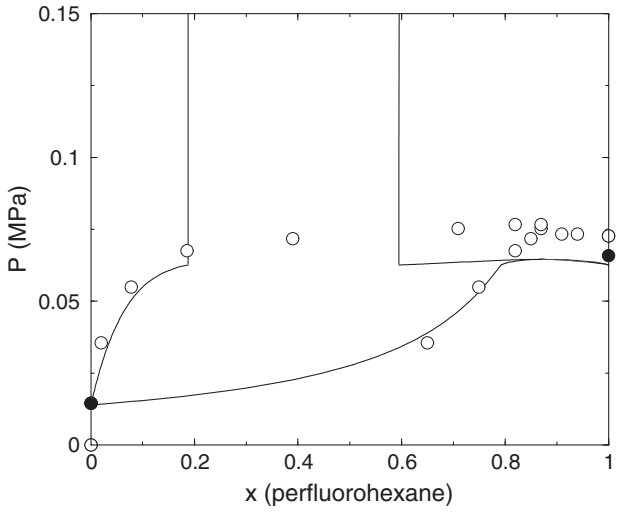

Fig. 5. An isothermal pressure-composition slice of the vapour–liquid phase diagram of the *n*-heptane + perfluoro-*n*-hexane mixture at $T=317.65$ K. The open circles are the data obtained from direct molecular-dynamics simulation, and the continuous curves represent the predictions with the SAFT-VR EoS.

On the other hand, the SAFT-VR predictions for the VLE appear to show excellent agreement with experiment throughout this temperature range. The composition dependence of the excess molar volumes are also calculated from the molecular-dynamics simulations and the SAFT-VR EoS, and the results are shown in Fig. 3. As can be seen, the agreement between the theory, simulation and experiment is very good.

Although this represents the extent of experimental data available for the *n*-heptane + perfluoro-*n*-hexane mixture, Figs. 1 and 2 alone do not suffice to provide a good understanding of the global phase diagram of this mixture. Additional isothermal pressure-composition slices of the fluid-phase equilibria can provide further insight. Accordingly, *P-x* isotherms are predicted using both simulation and theory, and the resulting fluid phase diagrams for the regions of VLE and LLE are presented in Figs. 4–6. In this case the simulated pressure is calculated from the virial route for the bulk coexisting vapour phase [64].

At temperatures below the lower critical end point of the mixture [16], liquid–liquid separation is predicted at high pressures by both molecular simulation and the SAFT-VR EoS. Moreover, azeotropy is exhibited by the mixture (although this is not easily observable in the figures due to the scale). Agreement between the simulated data and SAFT-VR calculations is good at low compositions of perfluoro-*n*-hexane, though for higher compositions the two methods exhibit a slight disagreement. Unfortunately, to our knowledge no experimental *P-x* data for the VLE of the *n*-heptane + perfluoro-*n*-hexane mixture are available. The only available experimental data are the pure-component limits (vapour pressures) and, correspondingly, these are the only experimental points represented in the figures. From these, it can be observed that SAFT-VR provides a slightly better agreement for the pure components at subcritical temperatures. However, at a temperature of $T=317.65$ K one still predicts liquid–liquid phase separation at high pressure with the SAFT-VR EoS (Fig. 5). This is due to the overprediction of critical line of the mixture (as discussed earlier in relation to the overestimation of the critical temperature in Fig. 1). The same overestimate of the critical point is not found in the simulations, and as a result at high pressures and concentrations between 0.2 and

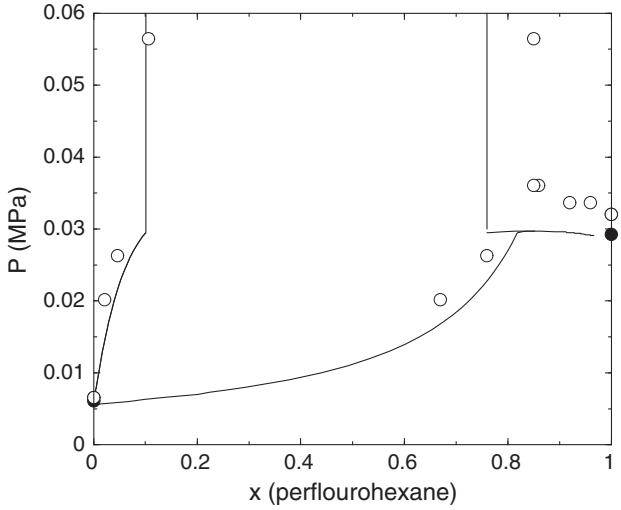

Fig. 4. An isothermal pressure-composition slice of the vapour–liquid phase diagram of the *n*-heptane + perfluoro-*n*-hexane mixture at $T=298.15$ K. The open circles are the data obtained from direct molecular-dynamics simulation, and the continuous curves represent the predictions with the SAFT-VR EoS.

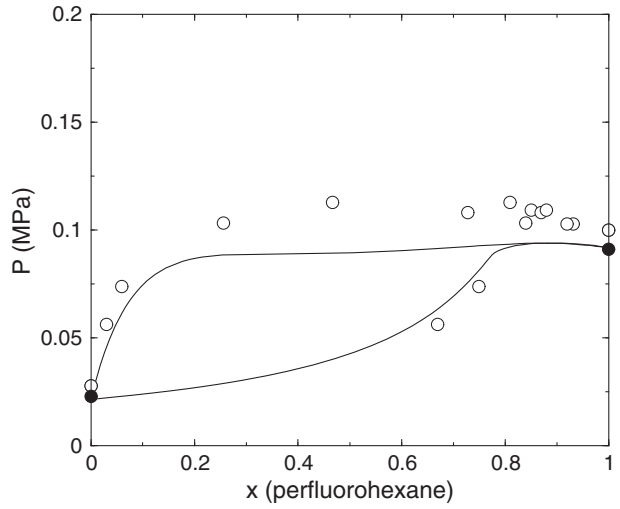

Fig. 6. An isothermal pressure-composition slice of the vapour–liquid phase diagram of the *n*-heptane + perfluoro-*n*-hexane mixture at $T=328.15$ K. The open circles are the data obtained from direct molecular-dynamics simulation, and the continuous curves represent the predictions with the SAFT-VR EoS.

0.6 the agreement between the SAFT-VR EoS and the simulation data is poor.

At $T = 328.15$ K (Fig. 6) the simulated data and the SAFT-VR calculations exhibit similar trends, though the simulation data is consistent with slightly higher coexistence pressures than predicted with the SAFT-VR EoS.

5.2. Interfacial tension

Liquid–liquid interfacial tensions are determined during the molecular-dynamics simulations using the test-area method as described in Section 4. As expected the interfacial tension γ exhibits a marked temperature dependence, tending to zero as the temperature approaches the critical value. The small magnitude of the values ($\gamma < 3$ mN/m) that we obtain for the liquid–liquid interface is a particularly notable feature, but unfortunately we did not find any experimental data with which to compare our results. In Fig. 7 the simulated data are correlated with the Eötvös [90] equation,

$$\gamma V_m^{2/3} = \kappa(T - T_c) \tag{11}$$

where κ is a constant (2.1×10^{-7} J/(K mol$^{-2/3}$)), V_m is the molar volume, and T_c is the critical temperature [90]. For pure components, the interfacial tension is found to be well represented by the Eötvös equation. We apply this relation merely as a guide to the eye. For these calculations the critical temperature is estimated to be $T_c = 316$ K as suggested by the experimental data; the molar volumes are evaluated empirically at each temperature.

A representative configuration of the liquid–liquid system, corresponding to the lower temperature data point of the figure (at $T = 273.15$ K), is also shown in Fig. 7. As is typical for such configurations, the system is not characterised by a sharp interface; rather the interface is slightly diffuse, as is consistent with the low value estimated for the liquid–liquid interfacial tension.

Vapour–liquid interfacial tensions of the system are also obtained during the course of the MD simulations. Experimental data for the vapour–liquid interfacial tension have been reported for the *n*-heptane + perfluoro-*n*-hexane mixture [3]. In Fig. 8 the vapour-liquid interfacial tensions at three different temperatures are shown as a function of the composition of the perfluoroalkane; the filled circles represent the experimental data while the open circles represent the simulated values.

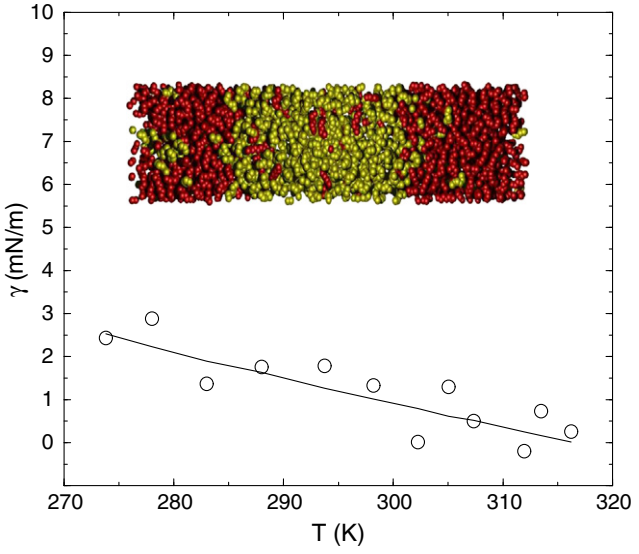

Fig. 7. The interfacial tension of the liquid–liquid interface of the *n*-heptane + perfluoro-*n*-hexane mixture as a function of temperature. The open circles are the data obtained from direct molecular dynamics simulation with the test-area method, and the continuous curve is an empirical correlation (see text). A snapshot of a typical configuration is shown (red represents the *n*-heptane molecules and yellow represents the perfluorohexane molecules).

At low composition of perfluoro-*n*-hexane the interfacial tension decreases rapidly until it exhibits a horizontal inflection corresponding to the onset of aneotropy [3].

To the best of our knowledge the term aneotropy was first used by McLure et al. [4] to refer to an inflection on the interfacial tension curves of a binary mixture as function of the concentration. Since then, the name has been used by other authors [87,91]. The inflection occurs for a perfluoro-*n*-hexane composition of $x_p \approx 0.2$ which appears to correspond to the inflection of the s-shaped curves for the vapour and liquid compositions (cf. Fig. 2) where there is a maximum in the composition of the vapour phase. At higher temperatures, near the critical composition x_c, the slope of the interfacial tension with composition $\left(\frac{\partial \gamma}{\partial x_p}\right)_T$ increases with the composition of the component with a higher interfacial tension, in agreement with the calculations with the square gradient theory [5,6]. At high perfluoro-*n*-hexane compositions, it can be seen that the simulation results deviate from the experimental data. Nevertheless, the simulated trends reflect qualitatively those exhibited in the experimental data.

6. Conclusions

In the present work a combined molecular-dynamics simulation and theoretical representation with the SAFT-VR EoS is employed to study the fluid phase equilibria and interfacial properties of the *n*-heptane + perfluoro-*n*-hexane binary mixture. The molecular simulations and theory are both seen to provide a good overall description of the vapour–liquid equilibria in comparison with the available experimental data, although the simulation values exhibit slightly larger deviations from experiment, in particular at high perfluoro-*n*-hexane compositions. The liquid–liquid immiscibility is of particular interest, since previous studies devoted to this interface are very limited. The general shape of the coexistence curve is correctly described using either methodology, and of reasonable quantitative accuracy in the low-temperature region. However, as expected, the use of the algebraic SAFT-VR EoS leads to an overestimate of the critical point, as the model parameters are adjusted to provide a good description away from the critical region. It is important to point out that any analytical (classical) equation of state is expected to fail close to the critical point as the description is characterised by a classical critical exponent of 1/2 rather than the universal renormalisation group value of 0.325. A specific renormalisation group procedure is required to treat the critical and near-critical region adequately, but this is beyond the scope of our current work. In the case of the simulations in the NVT or the NVE ensembles, finite-size effects also lead to an overestimate of the critical point. It would be possible to use extended critical scaling to extrapolate the data to the critical point [92,93], however, this was not the goal in this instance.

From simulations using the same values of the intermolecular parameters, we evaluate both vapour–liquid and liquid–liquid interfacial tensions of the *n*-heptane + perfluoro-*n*-hexane mixture; to the best of our knowledge these are the first reported liquid–liquid tensions for this mixture. The liquid–liquid interfacial tensions appear to exhibit the correct trends although some scatter is observed, presumably due to the closeness of the state points to the critical region. In terms of the vapour–liquid interface it was possible to capture the characteristic aneotropic behaviour of the experimental surface tension [44], i.e., a horizontal inflection for the near-critical isotherm. Moreover, from the simulations we observed that this mixture exhibits surface-tension isotherms of type 2, as classified and predicted by McLure et al. [3] with a negative surface tension-composition slope on approaching the critical point, x_c.

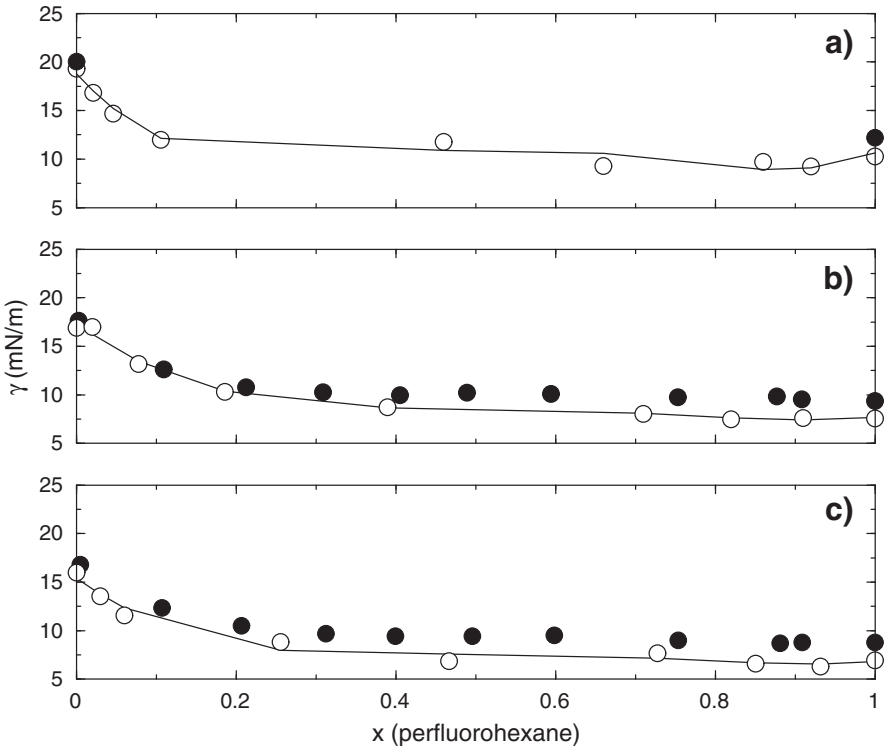

Fig. 8. The interfacial tensions of the vapour–liquid interface of the *n*-heptane + perfluoro-*n*-hexane mixture at a) $T = 298.15$ K, b) $T = 317.65$ K, and c) $T = 328.15$ K. The filled circles are the experimental data [3], and the open circles represent the data obtained from direct molecular-dynamics simulation with the test-area method. The continuous curve is included as a guide for the eye.

As a concluding statement we should emphasise that despite the simplicity of the force fields employed, the chosen interaction parameters of the models allows one to capture the basic features of both the vapour–liquid and liquid–liquid equilibria and the corresponding interfacial tensions of the binary mixture.

Acknowledgements

H.D. acknowledges support from DGAPA-UNAM, México and CONACyT Mexico for a sabbatical grant and grants from DGAPA IN102812 and CONACyT 154899. Additional funding from the Engineering and Physical Sciences Research Council (EPSRC) of the UK (grant no. EP/E016340) is also gratefully acknowledged by the Molecular Systems Engineering Group, as is the award of a refurbishment grant from the Royal Society–Wolfson Foundation.

References

[1] L. Lepori, E. Matteoli, A. Spanedda, C. Duce, M.R. Tiné, Fluid Phase Equilibria 201 (2002) 119.
[2] P. Morgado, C. McCabe, E.J.M. Filipe, Fluid Phase Equilibria 228 (2005) 389.
[3] I.A. McLure, R. Whitfield, J. Bowers, Journal of Colloid and Interface Science 203 (1998) 31.
[4] I.A. McLure, B. Edmonds, M. Lal, Nature Physical Science 241 (1973) 71.
[5] B. Widom, Journal of Chemical Physics 67 (1977) 872.
[6] F. Ramos-Gómez, B. Widom, Physica A 104 (1980) 595.
[7] J.H. Hildebrand, D.R.F. Cochran, Journal of the American Chemical Society 71 (1949) 22.
[8] J.H. Hildebrand, B.B. Fisher, H.A. Benesi, Journal of the American Chemical Society 72 (1950) 4348.
[9] D.N. Campbell, J.B. Hickman, Journal of the American Chemical Society 75 (1953) 2879.
[10] J.B. Hickman, Journal of the American Chemical Society 77 (1955) 6154.
[11] J.H. Simons, R.D. Dunlap, Journal of Chemical Physics 18 (1950) 335.
[12] J.H. Simons, J.W. Mausteller, Journal of Chemical Physics 20 (1952) 1516.
[13] J.H. Hildebrand, Journal of Chemical Physics 18 (1950) 1337.
[14] R. Dunlap, Journal of Chemical Physics 21 (1953) 1293.
[15] T.M. Reed, Journal of Physical Chemistry 63 (1959) 1798.
[16] J.S. Rowlinson, F.L. Swinton, Liquids and Liquid Mixtures, 3rd ed. Butterworth Scientific, London, 1982.
[17] E.A. Müller, K.E. Gubbins, Industrial and Engineering Chemistry Research 40 (2001) 2193.
[18] I.G. Economou, Industrial and Engineering Chemistry Research 41 (2002) 953.
[19] P. Paricaud, A. Galindo, G. Jackson, Fluid Phase Equilibria 194 (2002) 87.
[20] S.P. Tan, H. Adidharma, M. Radosz, Industrial and Engineering Chemistry Research 47 (2008) 8063.
[21] G.M. Kontogeorgis, G.K. Folas, Thermodynamic Models for Industrial Applications, Wiley, 2010. Ch. 8.
[22] C. McCabe, A. Galindo, SAFT associating fluids and fluids mixtures in: Applied Thermodynamics of Fluids, in: A.R.H. Goodwin, J.V. Sengers, C.J. Peters (Eds.), The Royal Society of Chemistry, London, 2010, pp. 215–279, Chapter 8.
[23] A.L. Archer, M.D. Amos, G. Jackson, I.A. McLure, International Journal of Thermophysics 17 (1996) 201.
[24] P.J. Clements, S. Zafar, A. Galindo, G. Jackson, I.A. McLure, Journal of the Chemical Society, Faraday Transactions 93 (1997) 1331.
[25] C. McCabe, A. Gil-Villegas, G. Jackson, The Journal of Physical Chemistry. B 102 (1998) 4183.
[26] C. McCabe, A. Galindo, A. Gil-Villegas, G. Jackson, International Journal of Thermophysics 19 (1998) 1511.
[27] C. McCabe, A. Galindo, A. Gil-Villegas, G. Jackson, The Journal of Physical Chemistry. B 102 (1998) 8060.
[28] C. McCabe, G. Jackson, Physical Chemistry Chemical Physics 1 (1999) 2057.
[29] E.J.M. Filipe, E.J.S. Gomez de Azevedo, L.F.G. Martins, V.A.M. Soares, J.C.G. Calado, C. McCabe, G. Jackson, The Journal of Physical Chemistry. B 104 (2000) 1315.
[30] E.J.M. Filipe, L.F.G. Martins, J.C.G. Calado, C. McCabe, G. Jackson, The Journal of Physical Chemistry. B 104 (2000) 1322.
[31] C. McCabe, L.M.B. Dias, G. Jackson, E.J.M. Filipe, Physical Chemistry Chemical Physics 3 (2001) 2852.
[32] E.J.M. Filipe, L.M.B. Dias, J.C.G. Calado, C. McCabe, G. Jackson, Physical Chemistry Chemical Physics 4 (2002) 1618.
[33] L.M.B. Dias, R.P. Bonifácio, E.J.M. Filipe, J.C.G. Calado, C. McCabe, G. Jackson, Fluid Phase Equilibria 205 (2003) 163.
[34] A.M.A. Dias, J.C. Pàmies, J.A.P. Coutinho, I.M. Marrucho, L.F. Vega, The Journal of Physical Chemistry. B 108 (2004) 1450.
[35] M.J. Pratas de Melo, A.M.A. Dias, M. Blesic, L.P.N. Rebelo, L.F. Vega, J.A.P. Coutinho, I.M. Marrucho, Fluid Phase Equilibria 242 (2006) 210.
[36] A. Tihic, G.M. Kontogeorgis, N. von Solms, M.L. Michelsen, Fluid Phase Equilibria 248 (2006) 29.
[37] M.C. dos Ramos, F. Blas, Molecular Physics 108 (2010) 1349.
[38] M. Schoen, C. Hoheisel, O. Beyer, Molecular Physics 58 (1986) 699.
[39] S. Brode, I.R. MacDonald, Molecular Physics 65 (1988) 1007.
[40] W. Song, P.J. Rossky, M. Maroncelli, Journal of Chemical Physics 119 (2003) 9145.

[41] L. Zhang, J.I. Siepmann, The Journal of Physical Chemistry. B 109 (2005) 2911.
[42] J.J. Potoff, D.A. Bernard-Brunel, The Journal of Physical Chemistry. B 113 (2009) 14725.
[43] C. Duce, M.R. Tinè, L. Lepori, E. Matteoli, Fluid Phase Equilibria 199 (2002) 197.
[44] R.A. Khairulin, S.V. Stankus, V.A. Gruzdev, V.A. Bityutskii, Russian Journal of Physical Chemistry A 83 (2009) 50.
[45] E. de Miguel, N.G. Almarza, G. Jackson, Journal of Chemical Physics 127 (2007) 034707.
[46] E.A. Müller, A. Mejía, Fluid Phase Equilibria 282 (2009) 68.
[47] F. Biscay, A. Ghoufi, V. Lachet, P. Malfreyt, Journal of Chemical Physics 131 (2009) 124707.
[48] F. Biscay, A. Ghoufi, V. Lachet, P. Malfreyt, The Journal of Physical Chemistry. B 113 (2009) 14277.
[49] C. Miqueu, J.M. Míguez, M.M. Piñeiro, T. Lafitte, B. Mendiboure, The Journal of Physical Chemistry. B 115 (2011) 9618.
[50] J. López-Lemus, M. Romero-Bastida, T.A. Darden, J. Alejandre, Molecular Physics 104 (2006) 2413.
[51] E. Díaz-Herrera, J. Alejandre, G. Ramírez-Santiago, F. Forstmann, Journal of Chemical Physics 110 (1999) 8084.
[52] I. Benjamin, Chemical Physics 180 (1994) 287.
[53] I. Benjamin, Annual Review of Physical Chemistry 48 (1997) 407.
[54] S. Senapati, M.L. Berkowitz, Physical Review Letters 87 (2001) 176101.
[55] L.X. Dang, Journal of Chemical Physics 110 (1999) 10113.
[56] S.E. Feller, Y. Zhang, R.W. Pastor, Journal of Chemical Physics 103 (1995) 10267.
[57] S. Iatsevitch, F. Forstmann, Journal of Physics: Condensed Matter 13 (2001) 4769.
[58] L. Frediani, C.S. Pomelli, J. Tomasi, Physical Chemistry Chemical Physics 2 (2000) 4876.
[59] F. Pierce, M. Tsige, D. Perahia, G.S. Grest, The Journal of Physical Chemistry. B 112 (2008) 16012.
[60] J. Gao, W.L. Jorgensen, Journal of Physical Chemistry 92 (1988) 5813.
[61] W. Shinoda, R. DeVane, M.L. Klein, Molecular Simulation 33 (2007) 27.
[62] D.G.A.L. Aarts, R.P.A. Dullens, H.N.W. Lekkerkerker, D. Bonn, R. van Roij, Journal of Chemical Physics 120 (2004) 1973.
[63] A. Mejía, J.C. Pàmies, D. Duque, H. Segura, L.F. Vega, Journal of Chemical Physics 123 (2005) 034505.
[64] M.P. Allen, D.J. Tildesley, Computer Simulation of Liquids, Clarendon Press, Oxford, 1987.
[65] S.K. Nath, F.A. Escobedo, J.J. de Pablo, The Journal of Chemical Physics 108 (1998) 9905.
[66] W.L. Jorgensen, J.D. Madura, C.J. Swenson, Journal of the American Chemical Society 106 (1984) 6638.
[67] S.T. Cui, J.I. Siepmann, H.D. Cochran, P.T. Cummings, Fluid Phase Equilibria 146 (1998) 51.
[68] G.H. Hudson, J.C. McCoubrey, Transactions of the Faraday Society 56 (1960) 761.
[69] A.E.H.N. Mousa, A. Kreglewski, W.B. Kay, The Journal of Chemical Thermodynamics 4 (1972) 301.
[70] C.M. Colina, A. Galindo, F.J. Blas, K.E. Gubbins, Fluid Phase Equilibria 222 (2004) 77.
[71] F. Kohler, J. Fischer, E. Wilhelm, Journal of Molecular Structure 84 (1982) 245.
[72] A.J. Haslam, A. Galindo, G. Jackson, Fluid Phase Equilibria 266 (2008) 105.
[73] T.R. Forester, W. Smith, http://www.ccp5.ac.uk/DL-POLY/. See also Smith, W.; Forester, T. R. Journal of Molecular Graphics 14 (1996) 136.
[74] W.G. Chapman, K.E. Gubbins, G. Jackson, M. Radosz, Fluid Phase Equilibria 52 (1989) 31.
[75] W.G. Chapman, K.E. Gubbins, G. Jackson, M. Radosz, Industrial and Engineering Chemistry Research 29 (1989) 1709.
[76] M.S. Wertheim, Journal of Statistical Physics 35 (1984) 19.
[77] M.S. Wertheim, Journal of Statistical Physics 35 (1984) 35.
[78] M.S. Wertheim, Journal of Statistical Physics 42 (1986) 459.
[79] M.S. Wertheim, Journal of Statistical Physics 42 (1986) 477.
[80] A. Gil-Villegas, A. Galindo, P.J. Whitehead, S.J. Mills, G. Jackson, A.N. Burgess, Journal of Chemical Physics 106 (1997) 4168.
[81] A. Galindo, L.A. Davies, A. Gil-Villegas, G. Jackson, Molecular Physics 93 (1998) 241.
[82] L.A. Davies, A. Gil-Villegas, G. Jackson, Journal of Chemical Physics 111 (1999) 8659.
[83] L.A. Davies, A. Gil-Villegas, G. Jackson, International Journal of Thermophysics 19 (1998) 675.
[84] T. Lafitte, D. Bessieres, M.M. Piñeiro, J.L. Daridon, Journal of Chemical Physics 124 (2006) 024509.
[85] R.P. Bonifácio, E.J.M. Felipe, C. McCabe, M.F.C. Gomes, A.A.H. Pádua, Molecular Physics 100 (2002) 2547.
[86] P. Paricaud, A. Galindo, G. Jackson, Industrial and Engineering Chemistry Research 43 (2004) 6871.
[87] J.S. Rowlinson, B. Widom, Molecular Theory of Capillarity, Clarendon, Oxford, 1982.
[88] G.J. Gloor, G. Jackson, F.J. Blas, E. de Miguel, Journal of Chemical Physics 123 (2005) 134703.
[89] L.D. Gelb, E.A. Müller, Fluid Phase Equilibria 203 (2002) 1.
[90] A.N. Kensington, The Physics and Chemistry of Surfaces, 3rd ed. Oxford University Press, 1941.
[91] A. Mejía, M. Cartes, H. Segura, Journal of Chemical Thermodynamics 43 (2011) 1395.
[92] L. Vega, E. de Miguel, L.F. Rull, G. Jackson, I.A. McLure, The Journal of Chemical Physics 96 (1992) 2296.
[93] F. del Rio, E. Avalos, R. Espindola, L.F. Rull, G. Jackson, S. Lago, Molecular Physics 100 (2002) 2531.